




A Petrov–Galerkin approach for the numerical analysis of soliton and multi-soliton solutions of the Kudryashov–Sinelnshchikov equation

H. Samy, W. Adel*, , I. Hanafy and M. Ramadan

*Corresponding author

Received 9 April 2024; revised 29 July 2024; accepted 30 July 2024

Hayah Samy

Department of Mathematics and Computer Sciences, Faculty of Science, Port-Said University, Egypt. e-mail: h.samy.aly.z@gmail.com

Waleed Adel

Laboratoire Interdisciplinaire de l'Universite Francaise d'Egypte (UFEID Lab), Universite Francaise d'Egypte, Cairo 11837, Egypt. Department of Mathematics and Engineering Physics, Faculty of Engineering, Mansoura University, Mansoura, 35516, Egypt. e-mail: waleed.ouf@ufe.edu.eg

Ibrahim Hanafy

Department of Mathematics and Computer Sciences, Faculty of Science, Port-Said University, Egypt. e-mail: ihanafy@hotmail.com

Moutaz Ramadan

Department of Mathematics and Computer Sciences, Faculty of Science, Port-Said University, Egypt. e-mail: motaz_ramadan@sci.psu.edu.eg

How to cite this article

Samy, H., Adel, W., Hanafy, I. and Ramadan, M., A Petrov–Galerkin approach for the numerical analysis of soliton and multi-soliton solutions of the Kudryashov–Sinelnshchikov equation. *Iran. J. Numer. Anal. Optim.*, 2024; 14(4): 1310–1335. <https://doi.org/10.22067/ijnao.2024.87548.1422>

Abstract

This study delves into the potential polynomial and rational wave solutions of the Kudryashov–Sinelnshchikov equation. This equation has multiple applications including the modeling of propagation for nonlinear waves in various physical systems. Through detailed numerical simulations using the finite element approach, we present a set of accurate solitary and soliton solutions for this equation. To validate the effectiveness of our proposed method, we utilize a collocation finite element approach based on quintic B-spline functions. Error norms, including L_2 and L_∞ , are employed to assess the precision of our numerical solutions, ensuring their reliability and accuracy. Visual representations, such as graphs derived from tabulated data, offer valuable insights into the dynamic changes of the equation over time or in response to varying parameters. Furthermore, we compute conservation quantities of motion and investigate the stability of our numerical scheme using Von Neumann theory, providing a comprehensive analysis of the Kudryashov–Sinelnshchikov equation and the robustness of our computational approach. The strong alignment between our analytical and numerical results underscores the efficacy of our methodology, which can be extended to tackle more complex nonlinear models with direct relevance to various fields of science and engineering.

AMS subject classifications (2020): 65N12; 65N30.

Keywords: Quintic B-spline; Finite element method; Error analysis.

1 Introduction

The concept of solitons has long been regarded as a captivating nonlinear phenomenon that has attracted significant attention from researchers across various scientific disciplines and technological fields. It can be defined as a self-reinforcing solitary wave possessing unique properties, such as maintaining its shape and speed during propagation, even when encountering obstacles or interacting with other waves. These remarkable features stem from the delicate balance between nonlinear and dispersive effects within the underlying physical system. With these pivotal characteristics, solitons find numerous applications across diverse domains. For instance, in the realm of optical fibers, solitons demonstrate the ability to propagate over long distances

without distortion, rendering them ideal for high-capacity data transmission [19, 6, 27]. Moreover, solitons have found utility in simulating nonlinear systems, such as the Maccari system [24], and in modeling Rossby waves in geophysical fluid mechanics within fluid dynamics [39]. Further exploration of potential applications of solitons can be found in [11] and references therein.

Nonlinear evolution equations (NLEEs) represent a category of mathematical equations capturing the temporal evolution of nonlinear phenomena spanning diverse scientific domains. These equations exhibit a strong association with solitons, as certain types of NLEEs accurately describe their behavior. Characterized by nonlinear terms capturing interactions and feedback among different variables or quantities, NLEEs have found wide-ranging applications in physics, biology, chemistry, and engineering. Prominent among these equations are the Korteweg–de Vries (KdV) equation [18], as discussed by Johnson [16]; the nonlinear Schrödinger equation, examined by Rabinowitz [29]; and the sine-Gordon equation, explored by Rubinstein [32], among others. Governing diverse physical phenomena, such as water waves, optical fibers, Bose–Einstein condensates, and magnetic materials, NLEEs hold significant importance. Given their wide-ranging applications, researchers have actively pursued analytical and numerical solutions for NLEEs. For instance, Hyder and Barakat [12] employed the improved Kudryashov method to obtain exact solutions for NLEEs. Additionally, Bildik and Deniz [4] adapted perturbation iteration techniques to simulate solutions for nonlinear Klein–Gordon equations. Gepreel [8] employed a range of algebraic methods to tackle the nonlinear $(1 + 1)$ Ito integral differential equation as well as the $(1 + 1)$ nonlinear Schrödinger equation. Ghanbari et al. [9] employed the Lie symmetry method to simulate solutions for Kawahara–KdV type equations, obtaining exact Jacobi elliptic solutions. In addition, Pal, Chatterjee, and Saha [28] employed the Darboux transformation method for simulating the multiple soliton solutions for the general Lax equation. These are only a few of the models that can be found to simulate the NLEEs, and others can be found in [5] and references therein.

On the other hand, numerical techniques have been employed to approximate solutions to such problems. For instance, the finite difference method has been applied to solve Caputo–Hadamard fractional differential

equations [10]. The literature abounds with extensive efforts in simulating soliton solutions for these problems, and further research in this area continues to flourish. One of the most important forms of these equations is the Kudryashov–Sinelnshchikov equation, first introduced in 2003 by Kudryashov and Sinelnshchikov; see [1]. This equation, belonging to the class of integrable equations, finds numerous applications in studying various physical phenomena [20]. It is considered a generalization of the well-known KdV equation, involving the interaction of dispersion and nonlinearity [15]. The study of the Kudryashov–Sinelnshchikov equation has led to the development of various analytical and numerical techniques, including the Painlevé test, Hirota bilinear method [14], and Darboux transformation [35]. This equation has garnered significant attention from researchers due to its rich mathematical structure and its ability to model a wide range of phenomena, including soliton dynamics, wave interactions, and nonlinear wave phenomena. In 2010, Kudryashov and Sinelnshchikov developed a nonlinear partial differential equation to describe pressure waves in liquid and gas bubble mixtures, considering liquid viscosity and heat transfer. Researchers continue to explore the properties and solutions of this equation to deepen our understanding of nonlinear dynamics and its implications in physics and related fields. For example, Ryabov [33] discovered a new exact solution for this type of equation using a modification of the truncated method. Additionally, Ak, Osman, and Kara [1] established polynomial and rational wave solutions for the Kudryashov–Sinelnshchikov equation. They validated these findings through the application of an appropriate numerical technique. Other methods for solving this equation may include the G/G' polynomial expansion method [23] and the fractional novel analytic method [36]. It should be noted that relatively little work has been done on solving this type of equation in the literature, which motivated our investigation into an accurate solution for such a model equation.

One of the recently adopted approaches for addressing analogous issues is the finite element method. This technique is recognized for its effectiveness and draws from classical methodologies like the Ritz method [21], Petrov–Galerkin method [18, 26], and the least squares method to approximate solutions for boundary value problems encountered in the theory of elliptic partial

differential equations. These methods have been extensively applied in solving complex engineering problems [40] and physics phenomena [25, 30]. The finite element method involves partitioning a complex geometry into smaller, simpler regions known as elements, which are interconnected by nodes. The governing equations are then solved for each element, and the solutions are combined to obtain an approximation of the solution for the entire system. This technique finds widespread use across various domains, including structural analysis [3], heat transfer [7], fluid dynamics [2], and electromagnetics [13]. Its versatility and flexibility render it a popular choice for solving complex problems in engineering and science. Moreover, it has been effectively employed in addressing problems of nonlinear behavior, including the bioheat model [34], two-sided space-fractional evolution equation [22], Allen–Cahn type phase-field model [38], and other diverse applications.

In this paper, we are interested in solving the nonlinear Kudryashov–Sinelshchikov equation in the following form:

$$U_t + \alpha UU_x + \beta U_{xxx} + \gamma(UU_{xx})_x + \rho U_x U_{xx} = 0, \quad (1)$$

where $U(x, t)$ is a field variable, and it is the unknown that is to be determined. In addition, $\alpha, \beta, \gamma, \rho$ are real parameters, and the subscripts shown are represented as differentiation concerning time and space respectively. Depending on the context of the simulated model, the variable $U(x, t)$ in this equation can represent different physical quantities of interest. In the field of fluid dynamics, $U(x, t)$ may describe the velocity, pressure, or free surface displacement of water waves, allowing researchers to analyze the formation and evolution of solitary waves and solitons. In plasma physics, $U(x, t)$ can be interpreted as the electric potential or the density of charged particles, providing insights into the nonlinear behavior of plasma waves, including ion-acoustic solitons. Moreover, in the domain of solid mechanics, $U(x, t)$ may correspond to the displacement or deformation of a solid material under the influence of nonlinear effects, with implications for the design of advanced nonlinear mechanical systems and wave-based nondestructive testing. By investigating the analytical and numerical solutions of the Kudryashov–Sinelshchikov equation, as presented in this study, researchers can deepen their understanding of the rich nonlinear phenomena underlying these diverse

physical applications. The solution to (1) will be discussed using the known B-spline finite element method. The B-splines, or basis splines, are mathematical functions widely used for approximating complex curves and surfaces. They are constructed by combining a set of piecewise polynomial functions, each defined over a small interval. The resulting function is continuous and smooth, with adjustable levels of curvature or smoothness. B-splines are crucial in computer-aided design, computer graphics, and computer vision, where they are used to represent and manipulate complex geometric shapes.

The novelty of the presented work lies within the following points:

1. The Kudryashov–Sinelshchikov equation is investigated in this work.
2. The solution is based on the Petrov–Galerkin finite element technique accompanied by the quintic B-splines as basis functions.
3. A Crank–Nicolson approach is employed for time and the B-spline for spatial discretization.
4. A detailed stability analysis using Von-Neumann stability is illustrated to prove that the scheme is unconditionally stable.
5. Numerical experiments are undertaken to verify that the method yields precise solutions, offering insights into the dynamics of the novel model.

The paper is organized as follows: Section 2 presents a detailed description of the proposed technique. In Section 3, the Crank–Nicolson technique is illustrated to reduce the proposed model (1), whereas Section 4 presents the initial state of the solution. Section 5 focuses on the stability analysis of the proposed algorithm. The main results of the collocation technique are presented in Section 6, and the final and concluding remarks, along with potential future work, are addressed in Section 7.

2 Petrov–Galerkin finite element technique

In this section, we will illustrate the main steps for solving model (1) using the Petrov–Galerkin finite element method. We first define model (1); throughout $[a, b]$ is a finite region with boundary conditions. Next, let a partition of

$[a, b]$ be $a = x_0 < x_1 < \dots < x_N = b$ by the equally spaced knots x_i and let quintic B-splines with knots at the points x_i , $0 < i < N$ be $\phi_i(x)$, where the set $\phi_{i-2}, \phi_{i-1}, \phi_i, \phi_{i+1}, \phi_{i+2}, \phi_{i+3}$ constitutes a series of splines, serving as the basis for functions sought within the finite region $[a, b]$. The solution approximation $U_N(x, t)$ for $U(x, t)$ is defined as follows:

$$U_N(x, t) = \sum_{i=-2}^{N+2} \phi_i(x) u_i(t), \quad (2)$$

where u_i represent time-dependent parameters that can be computed from boundary conditions,

$$U(a, t) = U(b, t) = 0, \quad U_x(a, t) = U_x(b, t) = 0. \quad (3)$$

The intervals $[x_i, x_{i+1}]$ are utilized to define finite elements with nodes positioned at x_i and x_{i+1} . Each element $[x_i, x_{i+1}]$ is spanned by six splines $(\phi_{i-2}, \phi_{i-1}, \phi_i, \phi_{i+1}, \phi_{i+2}, \phi_{i+3})$, which are expressed within a local coordinate system denoted by ζ , defined as $h\zeta = (x - x_i)$ where $h = x_{i+1} - x_i$ and $0 \leq \zeta \leq 1$. The approximate solution in the quintic B-spline collocation method can be expressed as a combination of quintic B-spline basis functions for the approximation of the space variables under consideration. The formulations for all these splines across the element $[x_i, x_{i+1}]$ are given by

$$\begin{aligned} \phi_{i-2} &= 1 - 5\zeta + 10\zeta^2 - 10\zeta^3 + 5\zeta^4 - \zeta^5, \\ \phi_{i-1} &= 26 - 50\zeta + 20\zeta^2 + 20\zeta^3 - 20\zeta^4 + 5\zeta^5, \\ \phi_i &= 66 - 60\zeta^2 + 30\zeta^4 - 10\zeta^5, \\ \phi_{i+1} &= 26 + 50\zeta + 20\zeta^2 - 20\zeta^3 - 20\zeta^4 + 10\zeta^5, \\ \phi_{i+2} &= 1 + 5\zeta + 10\zeta^2 + 10\zeta^3 + 5\zeta^4 - 5\zeta^5, \\ \phi_{i+3} &= \zeta^5. \end{aligned} \quad (4)$$

Outside the interval $[x_{i-3}, x_{i+3}]$, the spline $\phi_i(x)$ and its fifth derivatives are zero. When we utilize (4) to formulate equations based on the element parameters u_i^e , these curves serve as “shape” functions for the element. The $U_N(x, t)$ variation across the element $[x_{i-3}, x_{i+3}]$ is provided by

$$u^e(x, t) = \sum_{j=i-2}^{i+3} \phi_j(x) u_i(t). \quad (5)$$

The derivatives at the knots and the nodal value of $U_N(x, t)$ are represented in terms of the element parameters as demonstrated below:

$$\begin{aligned} U_i &= u_{i-2} + 26u_{i-1} + 66u_i + 26u_{i+1} + u_{i+2}, \\ hU_i' &= 5(u_{i+2} + 10u_{i+1} - 10u_{i-1} - u_{i-2}), \\ h^2U_i'' &= 20(u_{i-2} + 2u_{i-1} - 6u_i + 2u_{i+1} + u_{i+2}), \\ h^3U_i''' &= 60(u_{i+2} - 2u_{i+1} + 2u_{i-1} - u_{i-2}), \\ h^4U_i'''' &= 120(u_{i-2} - 4u_{i-1} + 6u_i - 4u_{i+1} + u_{i+2}). \end{aligned} \quad (6)$$

The dashes denote differentiation with respect to x . When the Petrov–Galerkin method is employed in (1) and by utilizing the weight functions $W(x)$, the outcome is

$$\int_b^a W (U_t + \alpha U U_x + \beta U_{xxx} + \gamma (U U_{xx})_x + \rho U_x U_{xx}) dx = 0. \quad (7)$$

Now, let us establish the corresponding element matrices. For the contribution of the standard element $[x_i, x_{i+1}]$, we acquire

$$\int_e W (u_t^e + \alpha u^e u_x + \beta u_{xxx}^e + \gamma (u^e u_{xx}^e)_x + \rho u_x^e u_{xx}^e) dx = 0, \quad (8)$$

$$\begin{aligned} & \sum_{i=l-2}^{l+3} \left(\int_{x_l}^{x_{l+1}} \phi_k \phi_i dx \right) u_i^e + \beta \sum_{i=l-2}^{l+3} \left(\int_{x_l}^{x_{l+1}} \phi_k \phi_i''' dx \right) u_i^e \\ & + \alpha \sum_{j=l-2}^{l+3} \sum_{i=l-2}^{l+3} \left(\left(\int_{x_l}^{x_{l+1}} \phi_i \phi_j' \phi_k dx \right) u_i^e \right) u_j^e \\ & + (\gamma + \rho) \sum_{j=l-2}^{l+3} \sum_{i=l-2}^{l+3} \left(\left(\int_{x_l}^{x_{l+1}} \phi_k \phi_i' \phi_j'' dx \right) u_i^e \right) u_j^e \\ & + \rho \sum_{j=l-2}^{l+3} \sum_{i=l-2}^{l+3} \left(\left(\int_{x_l}^{x_{l+1}} \phi_k \phi_i \phi_j''' dx \right) u_i^e \right) u_j^e = 0. \end{aligned} \quad (9)$$

The matrix form is constructed as

$$A^e \dot{u}^e + \beta B^e u^e + \alpha C^e u^{eT} u^e + (\gamma + \rho) u^{eT} D^e u^e + \gamma u^{eT} E^e u^e = 0, \quad (10)$$

where the dot represents differentiation with respect to time t , and

$$u^e = (u_{l-2}, u_{l-1}, u_l, u_{l+1}, u_{l+2}, u_{l+3})^T. \quad (11)$$

The element matrices are given by

$$\begin{aligned} A_{ij}^e &= \int_{x_i}^{x_{l+1}} \phi_k \phi_i dx, & B_{ij}^e &= \int_{x_i}^{x_{l+1}} \phi_k \phi_i''' dx, & C_{ij}^e &= \int_{x_i}^{x_{l+1}} \phi_i \phi_j' \phi_k dx, \\ D_{ij}^e &= \int_{x_i}^{x_{l+1}} \phi_k \phi_i' \phi_j'' dx, & E_{ij}^e &= \int_{x_i}^{x_{l+1}} \phi_k \phi_i \phi_j''' dx, \end{aligned} \quad (12)$$

where i, j , and k range from $l - 2$ to $l + 3$ for the element $[x_l, x_{l+1}]$. Consequently, the matrices A^e and B^e are of size 6×6 , while C^e, D^e , and E^e are of size $6 \times 6 \times 6$. In our algorithm, instead of C^e, D^e , and E^e , we employ the corresponding 6×6 matrices c^e, d^e , and e^e .

$$C_{ij}^e = \sum_{k=l-2}^{l+3} c_{ijk}^e u_k^e, \quad D_{ij}^e = \sum_{k=l-2}^{l+3} d_{ijk}^e u_k^e, \quad E_{ij}^e = \sum_{k=l-2}^{l+3} e_{ijk}^e u_k^e. \quad (13)$$

This is contingent on the variables u_k^e . The matrices of elements A^e and B^e are algebraically determined from (12), where u_k^e is provided by (11). The equation below is derived by assembling the elements from (10).

$$A\dot{u} + (\beta B + \alpha C + (\gamma + \rho)D + \gamma E)u = 0, \quad (14)$$

where the matrices A, B, C, D, E are constructed from the element matrices A^e, B^e, C^e, D^e, E^e , respectively, in the usual way and

$$u = (u_{-2}, u_{-1}, u_0, \dots, u_{N+1}, u_{N+2})^T. \quad (15)$$

In the next section, we will illustrate the Crank–Nicolson approach for simulating the solution for the main model.

3 Crank–Nicolson approach

In this section, we will demonstrate the time discretization for the system given by (14) using the Crank–Nicolson approach. The Crank–Nicolson technique is a finite difference method utilized for numerically solving partial differential equations such as the heat equation. Time is centered around $(n + \frac{1}{2})\Delta t$, where Δt denotes the time step. Subsequently, we employ the Crank–Nicolson method, in the following form

$$u = \frac{1}{2}(u^n + u^{n+1}), \quad \dot{u} = \frac{1}{\Delta t}(u^{n+1} - u^n). \quad (16)$$

Substituting (16) into (14), we obtain the recurrence relationship

$$\frac{A}{\Delta t}(u^{n+1} - u^n) + \frac{1}{2}(\beta B + \alpha C + (\gamma + \rho)D + \gamma E)(u^{n+1} + u^n) = 0, \quad (17)$$

and then

$$\begin{aligned} & \left(A + \frac{\Delta t}{2}(\beta B + \alpha C + (\gamma + \rho)D + \gamma E) \right) u^{n+1} \\ & = \left(A - \frac{\Delta t}{2}(\beta B + \alpha C + (\gamma + \rho)D + \gamma E) \right) u^n. \end{aligned} \quad (18)$$

In the system (18), the time indices are denoted by the superscripts n and $n + 1$. This system comprises $N + 1$ linear equations with $N + 5$ variables. To ensure a unique solution, an additional four conditions derived from the boundary conditions must be satisfied. These conditions can be used to eliminate $u_{-2}, u_{-1}, u_0, \dots, u_{N+1}$, and u_{N+2} from the recurrence relationships (18), resulting in an 11-banded $(N + 5) \times (N + 5)$ matrix equation.

During each time step, an inner iteration is executed to verify the convergence of the nonlinear term. The following outlines the iteration algorithm:

Initially, u^0 is known. The first approximation, u_1^1 to u , is computed using $u = u^0$ as per (16). Subsequently, the second approximation u_2^1 is obtained with $u = \frac{1}{2}(u^0 + u_1^1)$, followed by the third u_3^1 with $u = \frac{1}{2}(u^0 + u_2^1)$. Typically, we find that ten iterations are sufficient to obtain a reasonable approximation for u^1 in this initial stage.

To obtain a first approximation, denoted as u_1^{n+1} , for u^{n+1} in general, we use $u = u^n + \frac{1}{2}(u^n + u^{n-1})$. Subsequently, a second approximation u_2^{n+1} is obtained with $u = \frac{1}{2}(u^n + u^{n+1})$, and so forth. Typically, convergence is

After determining the initial vector u^0 as the solution of the undecadiagonal matrix (18), the system is solved using a Thomas algorithm [37].

5 Stability analysis

In this section, the Kudryashov–Sinelnshchikov equation represented by model (1) is amenable to stability analysis through Fourier transform techniques. Specifically, one can express the solution of the equation as a Fourier series expansion and substitute it back into the equation to obtain a system of algebraic equations for the Fourier coefficients [25]. By analyzing the solutions of these algebraic equations, one can determine the stability properties of the system in question [41]. We begin by applying the Fourier transform for the main problem, which results in the following form:

$$U_m^n = z^n e^{imkh}, \quad (23)$$

Here, z denotes the growth factor of the error in a typical mode of amplitude z_n , h represents the element size, and k indicates the mode number. By substituting the Fourier mode given in (23) into the system (18), we obtain the following equality:

$$\begin{aligned} & \left(A + \frac{\Delta t}{2}(\beta B + \alpha C + (\gamma + \rho)D + \gamma E) \right) z^{n+1} e^{i(m+1)kh} \\ & = \left(A - \frac{\Delta t}{2}(\beta B + \alpha C + (\gamma + \rho)D + \gamma E) \right) z^n e^{imkh}. \end{aligned} \quad (24)$$

Let $a = \left(A + \frac{\Delta t}{2}(\beta B + \alpha C + (\gamma + \rho)D + \gamma E) \right)$ and $b = \left(A - \frac{\Delta t}{2}(\beta B + \alpha C + (\gamma + \rho)D + \gamma E) \right)$. Then (24) took the form

$$az^{n+1} e^{i(m+1)kh} = bz^n e^{imkh}, \quad (25)$$

for more simplicity, we divide both sides by $z^n e^{im\theta}$, where $\theta = kh$ so that the equation would be

$$aze^{i\theta} = b. \quad (26)$$

We obtain growth factor as follows:

$$z = \frac{b}{ae^{i\theta}}, \quad (27)$$

where $e^{i\theta} = \cos(\theta) + i\sin(\theta)$. As $|z| < 1$, then the scheme is unconditionally stable.

6 Computational results

In this section, we present the computational results to validate the theoretical findings. The numerical algorithm developed in Section 3 will be validated through the examination of test problems involving the migration and interaction of solitons. We utilize the L_2 and L_∞ error norms to quantify the disparity between the numerical and analytical solutions, thereby demonstrating the predictive accuracy of the scheme regarding the position and amplitude of the solution as the simulation progresses. The L_2 and L_∞ norms of the solution are defined as follows:

$$\begin{aligned} L_2 &= \|U^{exact} - U^n\|_2 = \left[h \sum_{i=1}^N |U_i^{exact} - U_i^n|^2 \right]^{\frac{1}{2}}, \\ L_\infty &= \|U^{exact} - U^n\|_\infty = \max_i |U_i^{exact} - U_i^n|. \end{aligned} \quad (28)$$

The Kudryashov–Sinelshchikov (1) has two conserved quantities, which are as follows:

$$\begin{aligned} C_1 &= \int_a^b u dx \simeq h \sum_{i=1}^N U_j^n, \\ C_2 &= \int_a^b \left[\frac{1}{(\gamma + \sigma)} \left((\gamma u + \beta^{\sigma\gamma+1} - \beta^{\sigma\gamma+1} \gamma^{-\sigma\gamma}) \right) \right] dx \\ &\simeq h \sum_{i=1}^N \left[\frac{1}{(\gamma + \sigma)} \left((\gamma u_j^n + \beta^{\sigma\gamma+1} - \beta^{\sigma\gamma+1} \gamma^{-\sigma\gamma}) \right) \right]. \end{aligned} \quad (29)$$

First, we give the case of a single solitary wave.

6.1 Single solitary wave

The exact solution to the Kudryashov–Sinelshchikov equation is of the form

$$U(x, t) = A \operatorname{sech}^2 \left[B(x - x_0 - ct) \right], \quad (30)$$

and the initial condition can take the following equation:

$$U(x, 0) = A \operatorname{sech}^2 \left[B(x - x_0) \right], \quad (31)$$

where $A = \frac{3\beta k^2 \mu^2}{\alpha - \gamma k^2 \mu^2}$, $B = \frac{k\mu}{2}$, and $c = \beta k^2 \mu^2$. The constants are in the form $\alpha = 1.5, \beta = 1.7, \gamma = 0.8, \sigma = 2.4, c = -2.4, k = 1, \mu = 0.5$. Three experiments were carried out: the first at $\Delta t = h = 0.1$, the second at $\Delta t = h = 0.025$, and the third at $\Delta t = 0.025, h = 0.1$. The error norms and conserved quantities are determined for various h and Δt values up to time $t = 20$.

For the first example, the algorithm is executed within the calculation range $[-100, 100]$ up to time $t = 20$ to demonstrate the proper functioning of our numerical technique. During the simulation calculations, typical values of $\Delta t = 0.1$ and $\Delta t = 0.025$ are employed, along with $h = 0.1$ and $h = 0.025$. Tables 1 and 2 present the values of the error norms and invariants at various time levels, enabling us to promptly discern the impact of the number of grid points on the numerical technique. As observed from the tables, the two conserved quantities remain nearly constant over time. Moreover, the computed values of the error norms are determined to be sufficiently small, with these errors scarcely altering over time.

Table 1: Error norms and conservative quantities single solitary wave at $\Delta t = h = 0.1$

t	L_2	L_∞	C_1	C_2
5.0	3.52322809e-04	1.114142546e-03	7.84615390357	-12.36234575240
10.0	3.52312669e-04	1.114034293e-03	7.84615401202	-12.36234573439
15.0	3.52288576e-04	1.114034292e-03	7.846154326030	-12.36234568224
20.0	3.52300820e-04	1.114034292e-03	7.84615523469	-12.36234553134

Additionally, Table 3 presents a comparison with earlier methods, specifically method one (finite element method with quintic B-spline, FEMQB-spline) [1] and method two (finite element method with septic B-spline, FEMSB-spline) [17] at time $t = 20$. It can be observed from the table that the error norms obtained using the current method align well with those ob-

Table 2: Error norms for the Kudryashov–Sinelnshchikov equation’s single solitary wave when $\Delta t = h = 0.025$

t	L_2	L_∞	C_1	C_2
5.0	2.3295e-08	4.5041e-10	1.4657e-07	-3.345103498
10.0	1.7861e-08	5.8745e-10	1.1238e-07	-3.34510350
15.0	1.3694e-08	7.6617e-10	8.6166e-08	-3.345103508
20.0	1.0500e-08	9.9928e-10	6.6066e-08	-3.345103511

tained using the earlier methods.

Table 3: Error norms for the Kudryashov–Sinelnshchikov equation’s single solitary wave when $\Delta t = h = 0.025$

t	Present Method		FEMQB-spline [1]		FEMSB-spline [17]	
	L_2	L_∞	L_2	L_∞	L_2	L_∞
5.0	2.3295e-08	4.5041e-10	3.4853e10-6	1.4600e10-6	3.1100e-06	1.3154e-06
10.0	1.7861e-08	5.8745e-10	5.7917e10-6	2.1598e10-6	5.7796e-06	2.0899e-06
15.0	1.3694e-08	7.6617e-10	1.2314e10-5	5.8342e10-6	1.2013e-05	5.4335e-06
20.0	1.0500e-08	9.9928e-10	2.2657e10-5	1.0635e10-5	2.2673e-05	1.0848e-05

Table 4 demonstrates that the error norms (L_2 and L_∞) and the two conserved quantities remain stable and consistent across different time values (t), which suggests that the numerical method used for solving the Kudryashov–Sinelnshchikov equation’s single solitary wave is reliable and maintains accuracy over time.

Figure 1 illustrates the two-dimensional states of the bell-shaped solitary wave solutions at time $t = 30$ seconds, along with the distribution of numerical errors at the same time for $h = \Delta t = 0.1$. Figure 2 presents the three-dimensional states of the bell-shaped solitary wave solutions obtained from $t = 0$ to $t = 20$. Additionally, the contour lines depicting the movement of each individual wave are visible in Figure 2. Figure 3 illustrates how the wave has changed over time. These visualizations demonstrate that the

Table 4: Error norms for the Kudryashov–Sinelschikov equation’s single solitary wave when $\Delta t = 0.025$, $h = 0.1$

t	L_2	L_∞	C_1	C_2
5.0	3.80470850877e-04	12.03154472e-04	7.84615382769	-12.36234576810
10.0	3.80458787872e-04	12.03116325e-04	7.84615382159	-12.36234576911
15.0	3.80358154750e-04	12.0279809e-04	7.84615381376	-12.36234577041
20.0	3.80461773590e-04	12.0312576e-04	7.84615380362	-12.3623457721

method under examination accurately captures the propagation movement of a single wave while preserving its amplitude and shape.

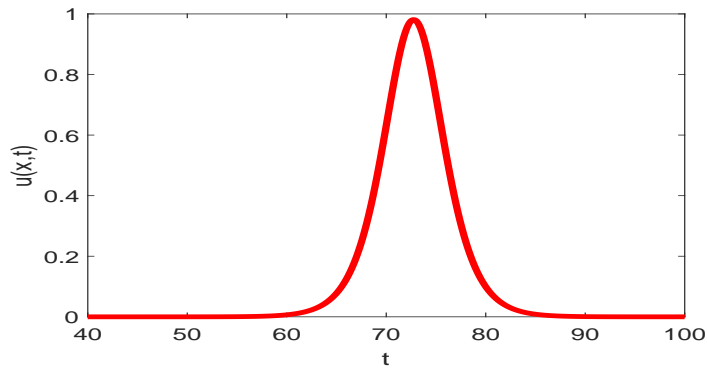


Figure 1: Behavior of numerical solution for $t = 30$.

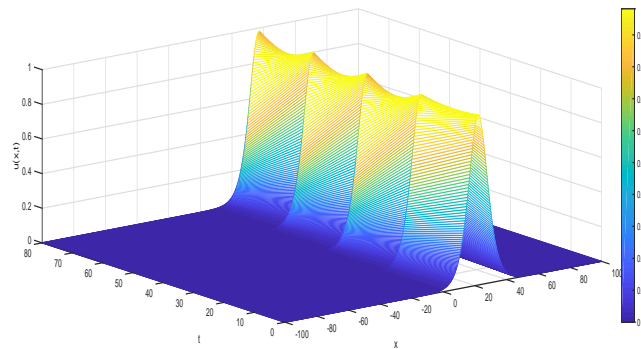


Figure 2: Space plot of one soliton solution for $t \in [0, 80]$.

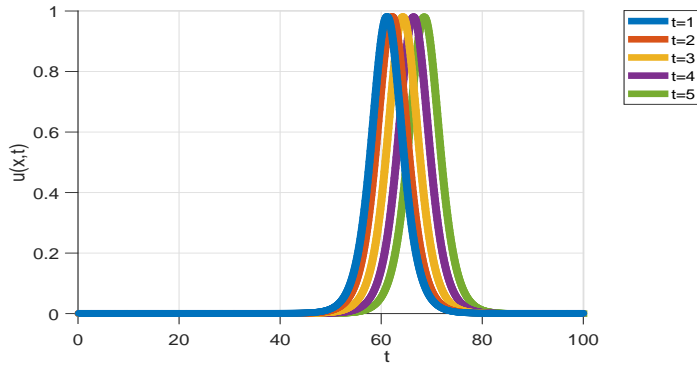


Figure 3: Behavior of numerical solution for $t \in [1, 5]$.

6.2 Interaction of two solitary waves

The interaction of two solitary waves moving in the same direction is investigated by utilizing an initial condition obtained from the linear sum of two well-separated solitary waves with distinct amplitudes. This initial condition can take the following form

$$U(x, 0) = \sum_{i=1}^2 A_i \operatorname{sech}^2 \left[B_i (x_i - x_0) \right]. \tag{32}$$

The collision of two solitary waves is analyzed in this problem using the following exact solution:

$$U(x, t) = \sum_{i=1}^2 A_i \operatorname{sech}^2 \left[B_i (x_i - x_0 - c_i t) \right], \tag{33}$$

where $A_i = \frac{3\beta k^2 \mu_i^2}{\alpha - \gamma k^2 \mu_i^2}$, $B_i = \frac{k\mu_i}{2}$, and $c_i = \beta k^2 \mu_i^2$. The constants are in the form $\alpha = 1.5, \beta = 1.7, \gamma = 0.8, \sigma = -2.4, c_1 = 0.833, c_2 = 0.425, k = 1, \mu_1 = 0.7, \mu_2 = 0.5$. Two experiments were carried out: the first at $\Delta t = h = 0.1$ and the second at $\Delta t = h = 0.025$.

To validate the proper functioning of our numerical technique, the algorithm is executed within the calculation range $[-100, 100]$ up to time $t = 20$ in this initial example. The values of the error norms and invariants for various time levels are presented in Table 5. This allows us to promptly assess

the impact of the number of grid points on the numerical technique. The table indicates that the two conserved quantities remained nearly consistent over time. Moreover, the computed error norm values are determined to be appropriately small, with these errors hardly ever changing over time. Additionally, Table 6 compares this method with the older method finite element method with septic B-spline (FEMSB-spline) [17] at time $t = 20$. Furthermore, Tables 7 and 8 illustrate how the double solitary wave has evolved as have changed $\Delta t = h = 0.025$ then $\Delta t = h = 0.1$. It can be observed from the table that the error norms calculated using the current method are consistent with those obtained using the older method.

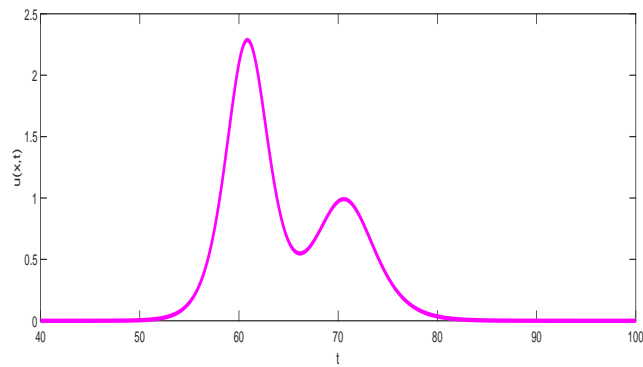


Figure 4: Behavior of numerical solution at $t = 25$ seconds.

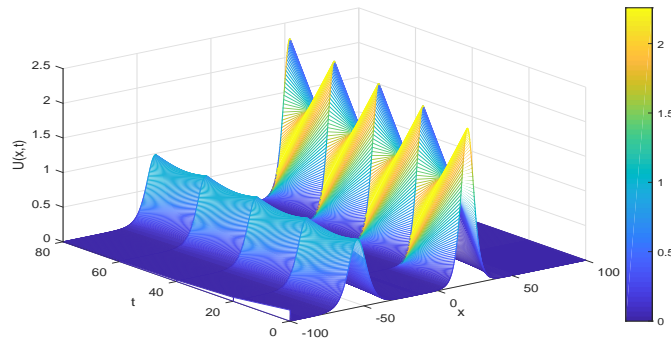


Figure 5: Numerical solution for $x \in [-100, 100]$ and $t \in [0, 80]$.

Figure 4 depicts the two-dimensional states of the bell-shaped solitary wave solutions at time $t = 25$ seconds, as well as the numerical error distri-

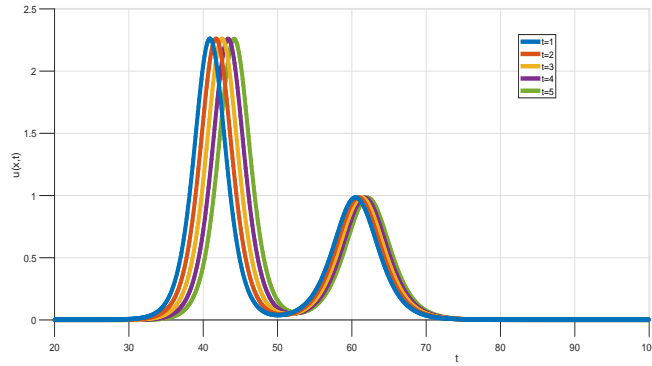


Figure 6: Behavior of numerical solution for $t \in [1, 5]$.

bution for $h = \Delta t = 0.1$ at time $t = 30$ seconds. Figure 5 shows that at time zero, the higher energy single wave lags behind the lower energy second wave. Depending on their magnitude, both waves flow to the right. More energy equals faster, according to solitary wave theory. Figure 6 illustrates how the wave has changed over time. As a result, the larger wave eventually reaches the smaller one, causing interference. Over time, the wave with the most energy leaves the second wave with the least energy, and solo waves finally revert to their initial form.

Table 5: Error norms for the Kudryashov–Sinelschikov equation’s two solitary waves when $\Delta t = h = 0.1$

t	L_2	L_∞	C_1	C_2
5.0	11.49337207e-04	3.63452337e-03	20.7342405464	-11.0358676030
10.0	11.49282935e-04	3.63435175e-03	20.7342406546	-11.0387332828
15.0	11.50661291e-04	3.6387104977e-03	20.7342409686	-11.0458076846
20.0	11.52842423e-04	3.6456078414e-03	20.7342418772	-11.06220804894

7 Conclusion

In this study, we present a detailed and comprehensive investigation of the numerical solution of the Kudryashov–Sinelschikov equation using a numer-

Table 6: Error norms for the Kudryashov–Sinelnshchikov equation’s two solitary waves when $\Delta t = h = 0.1$

t	Proposed technique		FEMSB-spline [17]	
	C_1	C_2	C_1	C_2
5.0	20.7342405464	-11.0358676030	20.7343904	-24.400625
10.0	20.7342406546	-11.0387332828	20.734406	-24.400625
15.0	20.7342409686	-11.0458076846	20.734405	-24.400625
20.0	20.7342418772	-11.06220804894	20.734415	-24.400624

Table 7: Error norms for the Kudryashov–Sinelnshchikov equation’s two solitary waves when $\Delta t = h = 0.025$

t	L_2	L_∞	C_1	C_2
5.0	1.7674008765e-05	5.5890123084e-05	7.9329863569e-05	-3.34509034835
10.0	1.76740087654e-05	5.5890123084e-05	7.9329863569e-05	-3.34509034835
15.0	8.5319829343e-06	2.6980499030e-05	3.8304877651e-05	-3.34509716131
20.0	4.1201731071e-06	1.302913136e-05	1.8504767045e-05	-3.34510044952

Table 8: Error norms and conservative quantities single solitary wave at $\Delta t = h = 0.1$ and $\alpha = 111.5$

t	L_2	L_∞	C_1	C_2
5.0	4.1151810516e-06	1.301334510e-05	0.091644205	-13.36524688650
10.0	4.1147812099e-06	1.3012080696e-05	0.0916442067	-13.36524688629
15.0	4.1140013153e-06	1.3009614453e-05	0.09164421	-13.36524688568
20.0	4.1149242293e-06	1.301253296e-05	0.091644221	-13.36524688398

ical collocation approach through simulations to elucidate its behavior. The Kudryashov–Sinelshchikov equation is a nonlinear partial differential equation that can model the dynamics of various physical field variables, such as fluid velocity, wave amplitude, plasma density, or displacement/deformation in solid mechanics. Through the finite element approach, we meticulously present a diverse array of accurate solutions for this equation, which has direct relevance to the study of nonlinear wave propagation phenomena in these physical systems.

The validation of our method's effectiveness is substantiated through the utilization of a collocation finite element approach based on quintic B-spline functions. Error norms, including L_2 and L_∞ , serve as robust metrics for evaluating the precision of our numerical solutions, affirming the reliability of our approach. Valuable insights into the dynamic evolution of the equation over time and under varying parameters, enriching our understanding of its behavior, have been presented. Furthermore, our study delves into the computation of conservation quantities of motion and the investigation of numerical scheme stability using the Von Neumann theory, further bolstering the credibility of our findings.

Based on these findings, the congruence between our analytical and numerical results underscores the robustness and efficacy of our approach in comprehensively addressing the Kudryashov–Sinelshchikov equation. These findings not only contribute to the broader understanding of nonlinear partial differential equations but also offer promising avenues for future research endeavors, particularly in extending our techniques to tackle more complex models with direct physical applications in the areas of fluid dynamics, wave propagation, plasma physics, and solid mechanics.

Acknowledgements

The authors would like to convey their thanks to the Editor and Reviewers for the helpful comments and suggestions which improved the work.

References

- [1] Ak, T., Osman, M.S., and Kara, A.H. *Polynomial and rational wave solutions of Kudryashov–Sinelshchikov equation and numerical simulations for its dynamic motions*, J. Appl. Anal. Comput. 10(5), (2020), 2145–2162.
- [2] Ali, L., Liu, X., Ali, B., Mujeed, S., Abdal, S., and Mutahir, A. *The impact of nanoparticles due to applied magnetic dipole in micropolar fluid flow using the finite element method*, Symmetry, 12(4), (2020), 520.
- [3] Belhocine, A., and Abdullah, O.I. *Thermomechanical model for the analysis of disc brake using the finite element method in frictional contact*, Multiscale Science and Engineering, 2(1), (2020), 27–41.
- [4] Bildik, N., and Deniz, S. *New approximate solutions to the nonlinear Klein–Gordon equations using perturbation iteration techniques*, Discrete Continuous Dyn. Syst. Ser S, 13(3), (2020), 503–518.
- [5] Chettri, K., Tamang, J., Chatterjee, P., and Saha, A. *Dynamics of nonlinear ion-acoustic waves in Venus’ lower ionosphere*, Astrophys. Space Sci. 369(5), (2024).
- [6] El-shamy, O., El-barkoki, R., Ahmed, H.M., Abbas, W., and Samir, I. *Exploration of new solitons in optical medium with higher-order dispersive and nonlinear effects via improved modified extended tanh function method*, Alex. Eng. J. 68, (2023), 611–618.
- [7] Feng, Y.-Y., and Wang, C.-H. *Discontinuous finite element method applied to transient pure and coupled radiative heat transfer*, Int. Commun. Heat Mass Transf. 122, (2021), 105156.
- [8] Gepreel, K. A. *Analytical methods for nonlinear evolution equations in mathematical physics*, Mathematics, 8(12), (2020), 2211.
- [9] Ghanbari, B., Kumar, S., Niwas, M., and Baleanu, D. *The Lie symmetry analysis and exact Jacobi elliptic solutions for the Kawahara–KdV type equations*, Results Phys. 23, (2021), 104006.

- [10] Gohar, M., Li, C., and Li, Z. *Finite difference methods for Caputo–Hadamard fractional differential equations*, *Mediterr. J. Math.* 17(6), (2020), 194.
- [11] He, J.-H., Qie, N., and He, C.-H. *Solitary waves travelling along an unsmooth boundary*, *Results Phys.* 24, (2021), 104104.
- [12] Hyder, A.-A., and Barakat, M.A. *General improved Kudryashov method for exact solutions of nonlinear evolution equations in mathematical physics*, *Phys. Scr.* 95(4), (2020), 045212.
- [13] Jamshed, W. *Finite element method in thermal characterization and streamline flow analysis of electromagnetic silver-magnesium oxide nanofluid inside grooved enclosure*, *Int. Commun. Heat Mass Transf.* 130, (2022), 105795.
- [14] Jin, Y.-T., and Chen, A.-H. *Resonant solitary wave and resonant periodic wave solutions of the Kudryashov–Sinelshchikov equation*, *Phys. Scr.* 95(8), (2020), 085208.
- [15] Jisha, C.R., Dubey, R.K., Benton, D., and Rashid, A. *The exact solutions for Kudryashov and Sinelshchikov equation with variable coefficients*, *Phys. Scr.* 97(9), (2022), 095212.
- [16] Johnson, R.S. *Water waves and Korteweg–de Vries equations*, *J. Fluid Mech.* 97(04), (1980), 701.
- [17] Karakoc, S.B.G., Saha, A., Bhowmik, S.K., and Sucu, D.Y. *Numerical and dynamical behaviors of nonlinear traveling wave solutions of the Kudryashov–Sinelshchikov equation*, *Wave Motion*, 118, (2023), 103121.
- [18] Karakoc, S.B.G., Saha, A., and Sucu, D. *A novel implementation of Petrov–Galerkin method to shallow water solitary wave pattern and superperiodic traveling wave and its multistability: Generalized Korteweg–de Vries equation*, *Chin. J. Phys.* 68, (2020), 605–617.
- [19] Kruglov, V.I., and Triki, H. *Propagation of coupled quartic and dipole multi-solitons in optical fibers medium with higher-order dispersions*, *Chaos Soliton. Fract.* 172, (2023), 113526.

- [20] Kumar, S., Niwas, M., and Dhiman, S.K. *Abundant analytical soliton solutions and different wave profiles to the Kudryashov–Sinelshchikov equation in mathematical physics*, *J. Ocean Eng. Sci.* 7(6), (2022), 565–577.
- [21] Leissa, A. *The historical bases of the Rayleigh and Ritz methods*, *J. Sound Vib.* 287(4-5), (2005), 961–978.
- [22] Liu, H., Zheng, X., Wang, H., and Fu, H. *Error estimate of finite element approximation for two-sided space-fractional evolution equation with variable coefficient*, *J. Sci. Comput.* 90(1), (2022), 15.
- [23] Lu, J. (2018). *New exact solutions for Kudryashov–Sinelshchikov equation*, *Adv. Diff. Equ.* 2018(1), 374.
- [24] Ma, Y.-L., Wazwaz, A.-M., and Li, B.-Q. *Soliton resonances, soliton molecules, soliton oscillations and heterotypic solitons for the nonlinear Maccari system*, *Nonlinear Dyn.* 111(19), (2023), 18331–18344.
- [25] Mohebbi, A., and Dehghan, M. *High-order compact solution of the one-dimensional heat and advection–diffusion equations*, *Appl. Math. Model.* 34(10), (2010), 3071–3084.
- [26] Nakazawa, S. *Computational Galerkin methods*, *Comput. Methods Appl. Mech. Eng.* 50(2), (1985), 199–200.
- [27] Ozisik, M., Secer, A., Bayram, M., Cinar, M., Ozdemir, N., Esen, H., and Onder, I. *Investigation of optical soliton solutions of higher-order nonlinear Schrödinger equation having Kudryashov nonlinear refractive index*, *Optik*, 274, (2023), 170548.
- [28] Pal, N.K., Chatterjee, P., and Saha, A. *Solitons, multi-solitons and multi-periodic solutions of the generalized Lax equation by Darboux transformation and its quasiperiodic motions*, *Int. J. Mod. Phys. B*, (2023).
- [29] Rabinowitz, P.H. *On a class of nonlinear Schrodinger equations*, *Z. fur Angew. Math. Phys.*, 43(2), (1992), 270–291.
- [30] Ramadan, M., and Aly, H. *New approach for solving of extended KdV equation*, *Alfarama Journal of Basic & Applied Sciences*, (2022).

- [31] Rezaei, S., Harandi, A., Moeineddin, A., Xu, B.-X., and Reese, S. *A mixed formulation for physics-informed neural networks as a potential solver for engineering problems in heterogeneous domains: Comparison with finite element method*, *Comput. Methods Appl. Mech. Eng.* 401, (2022), 115616.
- [32] Rubinstein, J. *Sine-Gordon equation*, *J. Math. Phys.* 11(1), (1970), 258–266.
- [33] Ryabov, P.N. *Exact solutions of the Kudryashov–Sinelshchikov equation*, *Appl. Math. Comput.* 217(7), (2010), 3585–3590.
- [34] Saeed, T., and Abbas, I. *Finite element analyses of nonlinear DPL bio-heat model in spherical tissues using experimental data*, *Mechanics Based Design of Structures and Machines*, 50(4), (2022), 1287–1297.
- [35] Shaikhova, G., Kutum, B., Altaybaeva, A., and Rakhimzhanov, B. *Exact solutions for the (3+1)-dimensional Kudryashov–Sinelshchikov equation*, *J. Phys. Conf. Ser.* 1416(1), (2019), 012030.
- [36] Sultana, M., Arshad, U., Abdel-Aty, A.-H., Akgül, A., Mahmoud, M., and Eleuch, H. *New numerical approach of solving highly nonlinear fractional partial differential equations via fractional novel analytical method*, *Fract. Fract.* 6(9), (2022), 512.
- [37] Weickert, J., Romeny, B., and Viergever, M. *Efficient and reliable schemes for nonlinear diffusion filtering*, *IEEE Trans. Image Process.* 7(3), (1998), 398–410.
- [38] Yang, X., and He, X. *A fully-discrete decoupled finite element method for the conserved Allen–Cahn type phase-field model of three-phase fluid flow system*, *Comput. Methods Appl. Mech. Eng.* 389, (2022), 114376.
- [39] Yin, X., Xu, L., and Yang, L. *Evolution and interaction of soliton solutions of Rossby waves in geophysical fluid mechanics*, *Nonlinear Dyn.* 111(13), (2023), 12433–12445.
- [40] Yong, W., Zhang, W., Nguyen, H., Bui, X.-N., Choi, Y., Nguyen-Thoi, T., Zhou, J., and Tran, T.T. *Analysis and prediction of diaphragm wall*

deflection induced by deep braced excavations using finite element method and artificial neural network optimized by metaheuristic algorithms, Reliab. Eng. Syst. Saf., 221, (2022), 108335.

- [41] Zahra, W.K., Ouf, W.A., and El-Azab, M.S. *An effective scheme based on quartic B-spline for the solution of Gardner equation and Harry Dym equation*, Communications on Advanced Computational Science with Applications, 2016(2), (2016), 82–94.